

# An Algebraic Solution for Banding Artifact Removal in bSSFP Imaging

M. N. Hoff<sup>1</sup>, and Q-S. Xiang<sup>1,2</sup>

<sup>1</sup>Physics, University of British Columbia, Vancouver, British Columbia, Canada, <sup>2</sup>Radiology, University of British Columbia, Vancouver, British Columbia, Canada

**Introduction** Balanced steady state free precession (bSSFP) sequences in MRI efficiently generate high signal images. While bSSFP exhibits excellent refocussing of spins dephased by  $B_0$  magnetic field inhomogeneity, excessive interpulse phase evolution  $\theta$  yields signal nulls (bands) in images. Typically, successive RF pulses in the bSSFP pulse train are phase cycled by an angle  $\Delta\theta$  in order to spatially shift the bands. Band attenuation is then achieved through some form of image combination [1,2].

Previously, we presented a geometric cross-solution (GS) which employs four phase cycled images to eliminate banding artifacts [3]; an image was formed from the cross-point of lines connecting alternating data points in the complex plane. An alternative approach is to demodulate the system using algebra: here a  $\theta$ -independent magnetization expression is derived from the bSSFP magnetization formulae of four phase cycled images. The performance of GS, the new algebraic solution (AS), and a standard complex sum (CS) are compared.

**Theory** Eq(1) represents a convenient formulation of the complex bSSFP magnetization [4,5].  $\alpha$  is the flip angle, and T1 and T2 relaxation terms are given by  $E_1 = e^{-TR/T_1}$  and  $E_2 = e^{-TR/T_2}$ . Signal in the four phase cycled images (for  $k = 1 \rightarrow 4$ ,  $\Delta\theta_k = 0^\circ, 90^\circ, 180^\circ, 270^\circ$  respectively) is represented by four unique  $I_k$  expressions dependent on four parameters  $M$ ,  $E_2$ ,  $b$  and  $\theta$ . AS is found by solving for the  $\theta$ -independent magnetization  $M$  — see Eq(2). GS is given in Eq(3) [3].

**Methods** Both AS and GS were applied to simulated and MR phantom images. Data was simulated using Eq(1) with  $\alpha = 41^\circ$  and  $TR = 5\text{ms}$ . Tissue has  $T1 = 200\text{ms} \rightarrow 3000\text{ms}$ , and  $T2 = 40\text{ms} \rightarrow 3000\text{ms}$ . Accordingly,  $E_2 = [0.88, 0.92, 0.97, 0.99]$  was set horizontally, and  $b = [0.2, 0.4, 0.6, 0.75]$  was set vertically, yielding a matrix of 16  $E_2/b$  combinations. For each combination,  $\theta$  values were varied from  $-\pi$  to  $\pi$  (Fig.1A). Phantom data was generated using a 3D TrueFISP (bSSFP) sequence on a 1.5T Siemens Avanto scanner. The imaged water bottle held a Zimmer™ (Warsaw, IN) Co-Cr-Mo alloy hip prosthesis to provide field inhomogeneity. The four datasets were acquired with  $52 \times 3\text{mm}$  slices,  $\alpha = 70^\circ$ , and  $TE/TR = 1.9\text{ms}/3.8\text{ms}$  (Fig.2A). Data was processed pixel-by-pixel: complex signal values  $I_k$ , their real parts  $x_k$ , and imaginary parts  $y_k$  were input into Eq(2) and Eq(3) to calculate AS and GS. Additionally, CS and a 2<sup>nd</sup> pass AS for improved SNR [6] were computed. SNR was calculated regionally by dividing the mean signal by its standard deviation.

**Results** Fig.1 depicts one of the four simulated images, and the corresponding CS, GS, and AS — all with and without noise. Both GS and AS eliminate bands. Fig. 2 shows the four phantom images, CS, GS, AS, and an SNR-improved 2<sup>nd</sup> pass AS. The SNR values in red on images with noise show that GS consistently has the highest SNR, and CS and AS have relatively similar SNR. Fig.2D & E illustrate that the lack of coherent ripple artifacts in AS permits regional processing to elevate SNR. AS becomes unstable if the real and imaginary parts of the input images are swapped, whereas GS is unaffected by data swapping (not shown).

**Discussion** An algebraic solution to the bSSFP banding problem is formulated and compared with the recently introduced geometric solution. GS and AS have fundamental differences: unlike GS, AS requires absolute definition of its real and imaginary parts, coinciding with the sign of the "i"s in Eq(2). GS is more robust in noise, thanks to the cross-point's resilience to data variability. Both solutions remove banding and yield incoherent, non-ripple artifacts which permit regional SNR enhancement. This work inspires further optimization and investigation into bSSFP signal demodulation.

**References** [1] Zur *et al.*, MRM, 16:444-459, 1990.  
[4] Ernst & Anderson, Rev Sci Instrum, 37:93-102, 1966.

[2] Bangerter *et al.*, MRM, 51:1038-1047, 2004.  
[5] Lauzon & Frayne, Conc Mag Res, 34A(3):133-143, 2009.

[3] Xiang & Hoff, Proc. ISMRM, 18:74, 2010.  
[6] Xiang & An, JMRI, 7:1002-1015, 1997

$$I_k = M \frac{1 - E_2 e^{i(\theta + \Delta\theta_k)}}{1 - b \cos(\theta + \Delta\theta_k)} \quad M = \frac{M_0(1 - E_1) \sin \alpha}{1 - E_1 \cos \alpha - E_2^2(E_1 - \cos \alpha)} \quad (1)$$

$$b = \frac{E_2(1 - E_1)(1 + \cos \alpha)}{1 - E_1 \cos \alpha - E_2^2(E_1 - \cos \alpha)}$$

$$\text{AS} \quad M = \frac{I_1 I_3 (I_2 - I_4)(1+i) + I_2 I_4 (I_1 - I_3)(1-i)}{I_1 I_2 - I_3 I_4 + i(I_2 I_3 - I_1 I_4)} \quad (2)$$

$$\text{GS} \quad M = \frac{(x_1 y_3 - x_3 y_1)(I_2 - I_4) - (x_2 y_4 - x_4 y_2)(I_1 - I_3)}{(x_1 - x_3)(y_2 - y_4) + (x_2 - x_4)(y_3 - y_1)} \quad (3)$$

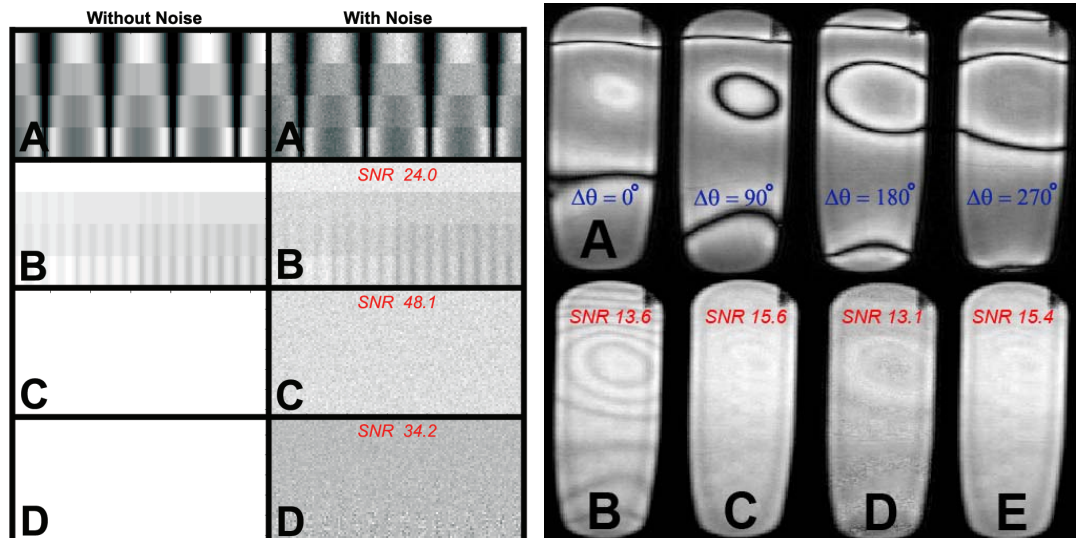


Fig.1: Simulated images without (left) and with (right) noise. A: One of four original datasets. B: Complex sum. C: Geometric solution. D: Algebraic solution.

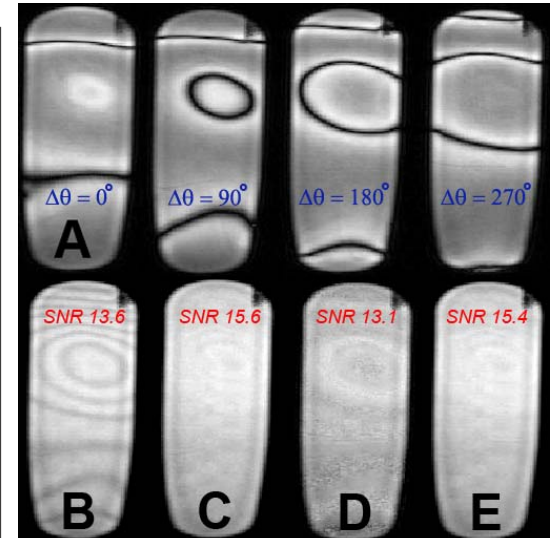


Fig.2: MR phantom images. A. Four phase cycled originals. B: Complex sum. C: Geometric solution. D: Algebraic solution (AS). E: SNR-enhanced AS.